Atmos. Chem. Phys. Discuss., 3, 2931–2962, 2003
www.atmos-chem-phys.org/acpd/3/2931/

Atmospheric Chemistry and Physics Discussions

Inelastic scattering in ocean water and its impact on trace gas retrievals from satellite data

M. Vountas, A. Richter, F. Wittrock, and J. P. Burrows

Institute for Environmental Physics, University of Bremen, Bremen, Germany

Received: 4 April 2003 – Accepted: 14 May 2003 – Published: 2 June 2003

Correspondence to: M. Vountas (vountas@iup.physik.uni-bremen.de)

Abstract

Over clear ocean waters, photons scattered within the water body contribute significantly to the upwelling flux. In addition to elastic scattering, inelastic Vibrational Raman Scattering (VRS) by liquid water is also playing a role and can have a strong impact on the spectral distribution of the outgoing radiance. Under clear-sky conditions, VRS has an influence on trace gas retrievals from space-borne measurements of the backscattered radiance such as from e.g. GOME (Global Ozone Monitoring Experiment). The effect is particularly important for geo-locations with small solar zenith angles and over waters with low chlorophyll concentration.

In this study, a simple ocean reflectance model (Sathendranath and Platt, 1998) accounting for VRS has been incorporated into a radiative transfer model. The model has been validated by comparison with measurements from a swimming-pool experiment dedicated to detect the effect of scattering within water on the outgoing radiation and also with selected data sets from GOME. The comparisons showed good agreement between experimental and model data and highlight the important role of VRS.

To evaluate the impact of VRS on trace gas retrieval, a sensitivity study was performed on synthetic data. If VRS is neglected in the data analysis, errors of about 36% are introduced for the slant column (SC) of BrO over clear ocean scenarios. The VRS-related error for the SC of HCHO is about 75%. Exemplarily DOAS retrievals of BrO from real GOME measurements including and excluding a VRS compensation led to comparable results as in the sensitivity study, but with somewhat smaller differences between the two analyses.

The results of this work suggest, that DOAS retrieval of atmospheric trace species from measurements of nadir viewing space-borne instruments have to take VRS scattering into account over waters with low chlorophyll concentrations, and that a simple correction term is enough to reduce the errors to an acceptable level.

ACPD

3, 2931–2962, 2003

1. Introduction

Backscattered light from waters with low concentrations of chlorophyll and gelbstoff – which are commonly referred to as oligotrophic waters – is significantly influenced by Vibrational Raman Scattering (VRS) within the water (e.g. Stavn and Weidemann, 1988; Marshall and Smith, 1990; Haltrin and Kattawar, 1993; Sathendranath and Platt, 1998; Vasilkov et al., 2002b).

As inelastic scattering redistributes photons over wavelength, VRS fills-in solar Fraunhofer lines, as well as trace gas absorption lines and therefore changes the spectral distribution of scattered light in the atmosphere. When measuring the backscattered radiance from space, this leads to stable spectral features over areas of the world's oceans. This is of particular importance for remote sensing from space as oligotrophic conditions prevail across large parts of the open ocean.

The impact of VRS on backscattered light is comparable to an atmospheric process, known as the *Ring effect* (Grainger and Ring, 1962). The origin of the Ring effect was found by several independent observations to be Rotational Raman Scattering (RRS) by O_2 and N_2 (e.g. Kattawar et al., 1981; Vountas et al., 1998, and references therein).

The effect of photon redistribution based on RRS influences atmospheric trace gas retrievals from measurements of backscattered light with space-borne instrumentation significantly (Vountas et al., 1998). Even if the contribution to the filling-in of redistributed photons by VRS in liquid water is usually smaller than the one by RRS in air it still has to be evaluated how large the impact on trace gas retrievals is.

Retrievals from data of the Global Ozone Monitoring Experiment (GOME) are potentially influenced by VRS. The GOME instrument was launched on ERS-2 in 1995 (Burrows et al., 1999). It is a nadir-viewing spectrometer taking backscatter measurements at moderate spectral resolution in the UV and visible spectral range. Global coverage is obtained in three days at the equator; the nominal swath is 960 km comprising three forward scans leading to a ground pixel size of 320 km (across track) x 40 km (along track).

ACPD
3, 2931–2962, 2003

Trace gas retrieval of GOME data typically uses the Differential Optical Absorption Spectroscopy (DOAS) method (Platt and Perner, 1980), whereby slant columns of atmospheric trace gases are fitted (and depending on the targeted species converted to vertical columns using a simulation of the Air Mass Factor). We have performed several DOAS investigations in different wavelength regions over various types of oceanic waters and found the effect of VRS to be most pronounced in the wavelength range between about 340 to 450 nm for oligotrophic waters.

Similar findings were reported in a recent paper by Vasilkov et al. (2002b). They were the first to show that VRS can have a significant impact on measurements of backscattered light from space-borne instrumentation. They showed good agreement between model results and GOME data and plan to use the resulting high-frequency spectral structures for chlorophyll retrieval.

In this study we incorporated a simple analytic oceanic reflectance model (developed by Sathendranath and Platt, 1998) in an atmospheric radiative transfer model (Rozanov et al., 1997; Vountas, 1998; Vountas et al., 1998; de Beek et al., 2001) to simulate accurately the upwelling radiance including the effect of VRS.

A first model verification was then performed by running the model for various scenarios (see Sect. 4) and comparing the results visually with those from Vasilkov et al. (2002b).

The model results are then validated using two approaches: (i) against spectra that have been measured directing one of our ground-based spectrometers directly to fresh water in a swimming pool (Sect. 5) and comparing up- and downwelling radiances; (ii) using GOME data measured over oligotrophic oceanic waters (Sect. 6).

Having successfully validated the model and its assumptions a sensitivity study is performed in order to quantify the isolated, theoretical error expected from neglecting the effects of VRS in the retrieval of trace gases using the DOAS technique. Finally we evaluate a number of selected GOME measurements and apply a VRS compensation spectrum (scheme) in order to estimate the impact of VRS on experimental data.

2. Historical background

This study was originally motivated by tests performed from one of us (F. Wittrock) on optimizing the wavelength window size for the DOAS-retrieval of OClO (Wittrock et al., 2000). Larger window sizes (357 nm towards 390 nm) led to large and stable fit residuals over oligotrophic waters that had a negative impact on the retrieval. Biologically more active regions of the oceans showed the effect to a much lesser degree as well as cloudy pixels that were not affected. Further tests with fresh water pixels from GOME (the great lakes in north America) also did not lead to a strong residual.

The upper map in Fig. 1 shows results from DOAS retrievals of GOME data over a period of one month (February) in 1999. All known trace gas absorptions and a Ring reference spectrum (Vountas et al., 1998) were fitted in the wavelength range of 345–385 nm. The upper map shows color-coded χ^2-values. High χ^2-values indicate a poor fit quality. Comparing geographical regions with high χ^2-values and areas having low chlorophyll-a concentrations derived from SeaWiFS data of the same month in 1999 (map below) show good qualitative agreement.

We concluded that the reason for this residual could be due to water-inherent characteristics. However, these characteristics must have been modulated with the Inherent Optical Properties (IOP) of natural waters, so that water rich in chlorophyll-a concentrations would lead to other residuals than oligotrophic water. Comparison of the regions with poor fitting results with those areas, where liquid water absorption can be detected in GOME measurements in the visible spectral region (Richter and Burrows, 2000) also suggested a link between average photon path in ocean water and the observed spectral structures.

In order to test this assumption, we set up an experiment pointing a spectrometer alternatively to the blue zenith-sky and the water of a clear fresh water swimming pool. From the two measurements, a residual was retrieved that was similar to that observed in the GOME data over clear water, demonstrating that the effect was indeed related to scattering on or in the water. The publication of Haltrin and Kattawar (1993); Sa-

thendranath and Platt (1998) and later Vasilkov et al. (2002b) pointed out that Raman scattering cannot be neglected in oligotrophic waters and leads to filling-in of solar Fraunhofer lines which could lead to effects as the one observed in our experiment. We therefore modeled the impact of Raman scattering on backscattered spectra and studied the resulting changes in the retrieved trace gas columns.

3. Modeling

The primary objective of both GOME and SCIAMACHY (Scanning Imaging Absorption Spectrometer for Atmospheric CHartographY) as well as forthcoming GOME-2 is to determine the abundances of atmospheric trace gases, such as O_3, NO_2, BrO, OClO, SO_2, HCHO, CH_4, CO, and N_2O. All these trace gases have narrow band absorptions, which can be utilized in the DOAS approach to derive their effective columns from the atmospheric optical depth. The main advantage of the DOAS retrieval is its high computational speed and the simplicity of the retrieval. Therefore, a possible correction of the effect of VRS on the data should also be simple and preferably have the form of a pseudo-absorber to be included in the fit. This approach is usually taken for the correction of atmospheric Raman scattering, and will here be employed for VRS as well.

Provided a DOAS-type retrieval a Differential Optical Depth (DOD) of the type DOD = $\ln(I/I_0) - P$, with I being the backscattered radiance, I_0 the extraterrestrial irradiance and P a polynomial, is evaluated. From this formalism we define a reference spectrum r_r accounting for RRS at a wavelength λ as:

$$r_r(\lambda) = \ln \frac{I^{+\mathrm{RRS}}(\lambda)}{I^{-\mathrm{RRS}}(\lambda)}. \quad (1)$$

With $I^{+\mathrm{RRS}}$ being the modeled radiance taking into account RRS and $I^{-\mathrm{RRS}}$ neglecting it (Vountas et al., 1998). Analogously we define a reference spectrum r_w accounting

ACPD
3, 2931–2962, 2003

for VRS in ocean water at a wavelength λ:

$$r_w(\lambda) = ln\frac{I^{+VRS}(\lambda)}{I^{-VRS}(\lambda)}. \quad (2)$$

In the following r_w is also called VRS compensation spectrum. I^{+VRS} is the modeled radiance taking into account VRS and I^{-VRS} the radiance neglecting it.

A prerequisite for taking into account VRS in DOAS-type retrievals is therefore a precise knowledge of the quantities I^{+VRS} and I^{-VRS}. This requires a coupled atmosphere-ocean radiative transport model, which is described in this section.

The oceanic model has been incorporated into an atmospheric model by simply passing the reflectance function for a given chlorophyll concentration to the atmospheric model which computes the radiance or flux for a given measurement geometry and atmospheric scenario.

The analytic oceanic reflectance model is based on the work of Sathendranath and Platt (1998). They found excellent agreement between results generated with their model and those of a relatively complex Monte-Carlo model. Despite this good agreement it should be noted that the model is based on several assumptions and simplifications: (i) the ocean surface is considered to be flat and the water column optically deep, i.e. no bottom effects have been taken into account; (ii) the IOP and mean cosines of the water are distributed uniformly in the water column; (iii) VRS contributes to the wavelength of interest through various source wavelengths: nevertheless all IOPs are computed for one representative source wavelength (see below for further discussion); (iv) The mean cosines are fixed to constant values (Vasilkov et al., 2002b); (v) only first order VRS is computed.

The result is a wavelength dependent reflectance function that is based on a bio-optical model having only the chlorophyll concentration as a one-parametric input. This assumption is valid whenever the concentration of phytoplankton is significantly larger than non-biogenic particles. Such waters are also referred to as *case I* waters (Morel and Prieur, 1977).

ACPD
3, 2931–2962, 2003

3.1. Oceanic model

The approach is based on seawater reflectance accounting for absorption and elastic, as well as inelastic (transspectral) scattering. Elastic scattering in water is dominated by Rayleigh scattering (or better "Einstein-Smoluchowski" scattering, referring to Mobley (1994) citing Young (1982)).

We adopt a model for the reflected light in the UV and visible wavelength range originally proposed by Sathendranath and Platt (1998) based on a modified Quasi-Single-Scattering Approximation (QSSA). The total reflectance $R(\lambda)$ at the *sea surface* including redistribution by VRS for a wavelength of interest λ is defined as:

$$R(\lambda) = R^E(\lambda) + R^R(\lambda) * \left[1 + \frac{b_b^E(\lambda)}{\kappa^E(\lambda)} + \frac{2b_b^E(\lambda')}{K(\lambda') + \kappa^E(\lambda')}\right] \quad (3)$$

λ' is a source wavelength which contributes photons (through Raman scattering) to the actual wavelength λ. The quantities R^E and R^R are the reflectances at sea surface attributed to elastic (superscript E) and inelastic, i.e. VRS (superscript R) light scattering (defined below). b_b^E is the backscattering coefficient for elastic scattering. Adopting the same terminology as Sathendranath and Platt (1998) we have defined K as the downward vertical attenuation coefficient and κ^E as the first-order elastic attenuation coefficient to be:

$$K(\lambda') = \frac{a(\lambda') + b_b(\lambda')}{\mu_d} \quad \text{and} \quad \kappa^E(\lambda') = \frac{a(\lambda') + b_b^E(\lambda')}{\mu_u^E}$$

Where μ_u^E is the mean cosine for the up-welling (elastic scattering only) and μ_d the one for the down-welling irradiance. a is the total absorption coefficient and b_b is the total backscattering coefficient. The reflectance formula part R^E is defined as:

$$R^E(\lambda) = \frac{s^E(\lambda) b_b^E(\lambda)}{\mu_d(\lambda)} * \frac{1}{K(\lambda) + \kappa^E(\lambda)}$$

ACPD
3, 2931–2962, 2003

where s^E is the so-called slope which was set to 1 (see original publication). The reflectance attributed to first-order VRS is defined by:

$$R^R(\lambda) = \frac{E_d(\lambda')}{E_d(\lambda)} * \frac{b_b^R(\lambda')}{\mu_d(\lambda')} * \frac{1}{K(\lambda) + \kappa^R(\lambda)}. \quad (4)$$

where b_b^R is the backscattering coefficient for VRS and the attenuation coefficient for first-order VRS is approximated by $\kappa^R = (a + b_b^E)/\mu_u^R$. $E_d(\lambda')$ and $E_d(\lambda)$ are the down-welling irradiance at sea surface for source and actual wavelength (λ', λ), respectively.

For Eq. (3) being valid it is necessary to have a vertically homogenous water body. The quantities required for the computation of $R(\lambda)$ are the apparent optical properties (AOP) μ_d, μ_u^R and μ_u which were set $\mu_d \approx 0.75$ (Sathendranath and Platt, 1998) and $\mu_u = \mu_u^R \approx 0.5$ (Vasilkov et al., 2002b). The determination of the down-welling flux E_d is done using SCIATRAN, the radiative transfer model described in Sect. 3.3.

The inherent optical properties, a, b_b^E and b_b^R and the corresponding wavelengths are discussed in the following Sect. 3.2.

3.2. Inherent optical properties of sea water

Apparent optical properties such as the reflectance as given by Eq. (3) require the knowledge of inherent optical properties (IOP) of the water body. With the exception of the VRS (back) scattering coefficient b^R which is determined through a simple exponential expression as a function of λ' both IOPs a and b_b will depend only on chlorophyll concentration C [mg/m^3]. This section describes how to determine all three quantities (IOPs).

The influence of VRS on GOME measurements is largest in case I water regions, where all inherent optical properties, except those of water itself, depend on phytoplankton concentration C. For estuarine and coastal waters (case II) the simple relationships found in case I waters do not hold and the contribution of detrital and dis-

solved organic matter (DOM) components to a is significantly larger than the one of phytoplankton.

Total Absorption Coefficient:

The total absorption coefficient a of a sea water body can be expressed as follows:

$$a(\lambda, C) = a_w(\lambda) + a_C(\lambda) + a_{\mathrm{DOM}}(\lambda).$$

Pure water absorption coefficients a_w were taken from wavelength spectral interpolation over two data sets ((Quickenden and Irvin, 1980) and Pope and Fry (1997)) as proposed by Vasilkov et al. (2002b).

a_C is the chlorophyll-related absorption coefficient taken from Vasilkov et al. (2002a) (data sets from personal communication).

According to the model of Morel (1988) the DOM absorption at 440 nm is 20% of the total absorption of pure seawater and particulate matter and an exponential function was used to describe the spectral variation of a_{DOM}:

$$a_{\mathrm{DOM}} = 0.2 * [a_w(440) + a_C(440)] * e^{-S*(\lambda-440)}$$

The spectral slope S of DOM was set to the wide-spread value of 0.014 nm^{-1} which, however is controversially discussed in literature (Vasilkov et al., 2002a; Patterson, 2000).

Total Elastic Backscattering Coefficient:

In order to compute Eq. 3 the total elastic backscattering coefficient b_b^E must also be known. A bio-optical model for this spectral quantity can be found in Morel (1988):

$$b_b(\lambda) = 0.5 b_w(\lambda) + \left[\, 0.002 + 0.02(0.5 - 0.25 \log C)\frac{550}{\lambda}\right] * \left[\, 0.3 C^{0.62} - b_w(550)\right]. \quad (5)$$

ACPD

3, 2931–2962, 2003

The pure sea water scattering coefficients b_w were taken from Smith and Baker (1981).

Backscattering Coefficients for VRS:

The mean wavenumber shift of 3357 cm^{-1} represents two fundamental OH stretch vibration modes of the water molecule that are further modified by hydrogen bonding and rotational fine structure. These interactions induce a broad band of emissions around the mean wavenumber shift so that water Raman emissions occur over a band of ≈ 30–50 nm. Walrafen (1967) showed that the spectral shape of measurements of Raman scattered intensities of pure water could be well reproduced by four different Gaussian functions. This empirical approach for calculating Raman scattering cross-sections was adopted by several authors devoted to this topic, for example Kattawar and Xu (1992) and Haltrin and Kattawar (1993). We have adapted the determination of the source wavelengths λ' from Haltrin and Kattawar (1993).

The values for the scattering coefficient b^R were determined using the following commonly used relation:

$$b^R(\lambda', \lambda) = b_0^R(\lambda'/\lambda_0)^P, \quad (6)$$

where b^R is the Raman scattering coefficient at wavelength λ' and $b_0^R = 2.610^{-4}$ m^{-1} is the Raman absorption coefficient at wavelength $\lambda_0 = 488$ nm. Bartlett et al. (1998) showed that the exponent P is near to 5.3 (instead of 5 as shown in older studies).

The phase function VRS is nearly isotropic (Ge et al., 1993) and leads to the simple relation between scattering and backscattering coefficient for VRS $b_b^R = 0.5b^R$ (required in Eq. 4).

3.3. Atmospheric model

Within the framework of this study the atmospheric model is necessary to provide the base for the incorporation of the oceanic reflectance function accounting for VRS. It is

ACPD
3, 2931–2962, 2003

furthermore necessary to determine the a priori unknown ratio of the down-welling irradiance E_d at λ and λ' as required in Eq. (4). From a formal point of view the reflectance (ocean) model provides the lower boundary condition of the atmospheric model.

The radiative transfer model used is SCIATRAN (formerly known as GOMETRAN) (Rozanov et al., 1997). The solution of the radiative transfer equation computed by SCIATRAN is based on the finite difference method and has been successfully validated against DISORT. The code calculates the complete unpolarized radiation field and irradiance for ground- or satellite viewing geometry for a given atmospheric composition with respect to the extra-terrestrial flux. The program also calculates appropriate weighting functions which are the response of the radiation field to a change of atmospheric parameters. The mathematical principles of the model are described in detail in Rozanov et al. (1997). The radiative transfer equation is evaluated in plane-parallel geometry, with the exception of the solar source function which is calculated in spherical geometry taking into account refraction. The model was extended to include inelastic scattering by RRS in the atmosphere and has been successfully validated and applied to remote sensing data (Vountas et al., 1998).

4. Model results

Figure 2 shows the percentage of filling-in in the wavelength range 340–400 nm. The filling-in was defined by $100 * (I^+ - I^-)/I^-$. Both spectra were prepared with the same atmospheric and geometric setup based on a solar spectrum measured by GOME. The VRS compensation spectrum was computed assuming a chlorophyll concentration of 0.01 [mg/m^3]. The solar zenith angle was set to 32° and a maritime Lowtran aerosol scenario (Kneizys et al., 1986) has been selected. The vertical distribution of trace gases, temperature and pressure was taken from the MPI climatology (Brühl and Crutzen, 1992) for October.

The Ring reference spectrum shows larger absolute spectral dynamics compared to the VRS compensations spectrum. We have checked the spectral correlation between

ACPD
3, 2931–2962, 2003

r_w and r_r by using a model approach: both spectra have been modeled for identical atmospheric and oceanic conditions and were fitted to each other in a DOAS-like fashion. In spite of a reasonable overall fit result there are still enough remaining differences to enable independent fitting of both spectra. This is a result of the different efficiencies of the processes and a much smaller spectral redistribution range of RRS about ± 2–3 nm in this wavelength region as compared to VRS which has an average shift of about 40 nm. We therefore conclude that the influence of VRS on DOAS retrievals even in small wavelength windows (< 10 nm) is not negligible because r_r cannot fully compensate the filling-in due to VRS (see below in Sect. 6). This fact can potentially be exploited for the determination of chlorophyll concentrations in sea water using DOAS retrievals.

The VRS spectrum is in good qualitative agreement with the results presented by Vasilkov et al. (2002b). However, they prepared their spectra on the basis of a slightly modified reflectance formula and used a four times lower spectral resolution as an input for their model. Therefore, a direct comparison has not been performed.

VRS spectra for other chlorophyll values C where also created. The overall behavior was similar to the results of Vasilkov et al. (2002b): The filling-in significantly increases with decreasing chlorophyll-a concentrations. This was expected because C governs the penetration depth and therefore the number of backscattered photons in case I waters. Vasilkov et al. (2002b) concluded from the strong interrelation between C and the magnitude of filling-in that chlorophyll-a concentrations can be retrieved from spectra of the backscattered light measured from satellite.

In an additional test, (fair weather) clouds were added to the SCIATRAN simulation. As a result, the effect reduces by three orders of magnitude for satellite geometry and can therefore be neglected. This is not surprising, as even optically thin clouds reflect a large part of the incoming light and therefore dramatically reduce the impact of upwelling radiation from water on space borne observations.

ACPD
3, 2931–2962, 2003

5. Swimming pool experiment

Historically the authors' assumptions on the origin of the residuals observed in GOME data was based on circumstantial evidence. The effect was not clearly identified and an instrumental artifact could not fully be excluded. In order to isolate the source of the observed structures, we have in spring 1999 performed measurements on the ground in Bremen, 53°N with one of our grating spectrometers usually employed for zenith-sky measurements. The spectral resolution of the instrument is comparable to the one of GOME in the UV channels; however, the spectral range covered is only 344 – 388 nm.

The instrument was set up on top of a 10 m high platform over the basin of a swimming pool that had been filled with fresh chlorinated water the day before. Light was fed into the spectrometer using a depolarizing quartz-fibre bundle attached to a small telescope with a narrow field of view (< 1°). The telescope was pointed alternatively to the blue sky and to the water surface which was shaded from direct sun in the field of view of the telescope to avoid interference from sun glint. During part of the measurements, a rotatable polarizer was mounted in the telescope and measurements were taken alternating between measurements in parallel and perpendicular polarization (with respect to the solar azimuth).

The sky was clear during the measurement period with some evidence for enhanced aerosol loading from the brightness of the horizon. The water in the basin was very clear and both the blue bottom and the sides of the basin were clearly visible indicating that at least in the visible spectral range, border effects can not be excluded.

When analyzing the results of the crossed-polarizer measurements in the way proposed by Solomon et al. (1987), the zenith-sky data produced a nice spectral Ring effect signature as expected for Rotational Raman scattered light. However, the nadir viewing measurements did not show such an effect, and very little difference was observed between the two polarisation directions. However, when upwards and downwards looking measurements were compared, a clear signature showed up that after subtraction of a polynomial was very similar to the residual structures observed in the

ACPD
3, 2931–2962, 2003

GOME measurements over clear ocean areas. We therefore concluded, that the observed features are not an instrumental artefact of GOME, but rather the result of a scattering or absorption effect of sun light in liquid water.

As a next step, we tried to simulate the swimming pool measurements with the VRS model developed in this study. The approach was to analyze the measured spectra using a simple DOAS approach and fitting an accurately modeled Ring r_r and VRS compensation r_w spectrum to the data.

r_r and r_w were computed according to the definitions in Eqs. (1) and (2). SCIATRAN was set up in a way that the conditions prevailing during the experiment could be taken into account as accurate as possible. $I^{\pm RRS}$ and $I^{\pm VRS}$ were computed with a highly sampled and resolved solar spectrum (Kurucz et al., 1984). The spectra were then smoothed and re-sampled to the instrument resolution and spectral spacing (full width at half maximum was 0.5 nm and average sampling was 0.16 nm).

Figure 3 shows the comparison of the fitted result for both spectra – VRS and RRS – and the corresponding residuals of the experimental spectrum. The agreement of modeled and fitted Ring spectrum r_r is slightly poorer than that of the VRS compensation spectrum r_w. The reasons for this behavior are still not fully understood. However, the overall agreement especially in case of the comparison of r_w is very good suggesting that the filling-in of Fraunhofer lines by VRS in liquid water is adequately modeled.

From the swimming pool experiment and the model calculations we conclude, that (i) VRS can have a significant impact on backscatter experiments and (ii) that our model can adequately model the effect of VRS on upwelling radiation over water surfaces in the UV. The next step was to analyze if the VRS compensation spectrum also fits well to the GOME measurements.

6. GOME

Both modeled spectra, the VRS compensation and Ring reference spectrum, were used within DOAS retrievals of GOME data in order to show their validity for remote

sensing data measured from GOME. Similar results are expected for SCIAMACHY (Scanning Imaging Absorption Spectrometer for Atmospheric CHartographY) once calibrated spectra are available.

Several DOAS fits of clear-sky GOME data measured over the Pacific ocean, near Easter island in February 1999, where low chlorophyll-a concentrations could be expected (see maps in Fig. 1) were performed. A wavelength window between 347 and 385 nm has been selected. The above described spectra (Ring reference and VRS compensation spectrum) were fitted in addition to the reference spectra of NO_2, O_4, BrO, O_3 (two spectra with different temperatures) and an under-sampling correction spectrum.

Small wavelength shifts due to tiny differences in the wavelength scale used in the VRS, Ring, cross-sections, GOME irradiance and radiance spectra are corrected by allowing a non-linear shift-and-squeeze of the wavelength axis for each spectrum relative to an arbitrary reference, here the GOME radiance.

The fit results are shown in Fig. 4. The comparison of the modeled Ring reference spectrum compared to the rest of the fit (except Ring effect contributions) is shown in the upper plot, the result for the modeled VRS compensation spectrum in the lower plot. Both reference spectra could nicely be identified in the data, indicating that the effects of VRS as predicted by the model are in fact observed in the DOD evaluated. A remaining apparent spectral feature is a *tripod* at about 383 nm which can be reproduced neither by the Ring reference nor by the VRS compensation spectrum.

It should be noted that prior to this study DOAS retrievals of measurements potentially influenced by VRS where performed using an empirical approach in order to reduce the impact of VRS.

7. Trace gas retrieval: case studies

Having demonstrated that VRS signatures are observable in GOME data over clear waters, and that our model provides an adequate simulation of the effect, we have

performed sensitivity studies to evaluate the effect of VRS on trace gas retrievals. A mixture of several different trace gas concentrations was used, each appropriate for the selected target species, Formaldehyde (HCHO) and Bromine Monoxide (BrO). For these scenarios, DODs have been modeled that include the effect of VRS. Using a standard DOAS retrieval, the modeled data have then been analyzed with and without applying a VRS compensation spectrum to determine the impact of VRS on the DOAS retrieval of the trace gas columns.

These tests should provide information on the theoretical accuracy if VRS is neglected in DOAS-like trace gas retrievals. For simplicity and clarity, instrumental characteristics have not been taken into account. The strategy involved only a few scenarios which however are representative for real space-borne measurements.

7.1. Strategy

Optical Depths OD = $ln(I/I_0)$ were computed using two atmospheric scenarios, based on the MPI climatology (Brühl and Crutzen, 1992) for October. However, for BrO and HCHO the trace gas amounts were increased by scaling the whole profile in order to rise the DOD for both gases to values that are routinely retrieved by GOME. Pressure, temperature and vertical profiles of all other trace gases remained unchanged. The solar irradiance I_0 was taken from Kurucz et al. (1984) and re-sampled to 0.2 nm. The first scenario differed from the second in solar zenith angle (SZA) and chlorophyll concentration: Scenario I: SZA=50°, C=0.01 [mg/m^3]; Scenario II: SZA=30°, C=0.001 [mg/m^3]. VRS increases with decreasing values of the SZA and C, hence significant differences for the impact of VRS for both scenarios are expected.

Radiances (for OD), VRS compensation spectra and Ring reference spectra were calculated on the same wavelength grid as the solar irradiance. All quantities were computed for scenario I and II using SCIATRAN. SCIATRAN's input spectra (trace gas absorption spectra etc.) were interpolated to the wavelength grid of the solar irradiance. In addition to molecular scattering processes (RRS and Rayleigh), aerosol scattering was also modeled assuming a maritime Lowtran aerosol scenario (Kneizys

et al., 1986).

The evaluation of the OD was performed with the DOAS method using the trace gas reference spectra involved in the previous modeling and various Ring and VRS compensation spectra. An OD for Scenario I and Scenario II was evaluated with the corresponding trace gas spectra and taking:

1. **adequate RRS and VRS spectra into account** to test for consistency and to use the resulting SC as the *true* reference,
2. **an adequate RRS but no VRS spectra into account** to show the isolated impact of neglecting VRS in the retrieval,
3. **no RRS spectrum but an adequate VRS spectrum into account** to test if the VRS spectrum is capable to compensate a missing RRS spectrum
4. **a non-adequate RRS spectrum and a non-adequate VRS spectrum into account** to test the realistic case of a retrieval using wrong a priori assumptions on the state of the atmosphere,

5-6. **an adequate RRS spectrum and a non-adequate VRS spectrum** as well as **an non-adequate RRS spectrum and an adequate VRS spectrum into account** to reveal the relative importance of the two processes.

Here, non-adequate spectra refer to computations using the wrong scenario, i.e. the OD has been computed for example for scenario I and the retrieval was performed using a RRS spectrum computed for scenario II.

The first step in this study was to perform test 1. and to retrieve a SC that served as a correct value SC_{true} (perfect fits are shaded grey in Fig. 5). All other tests (2-6.) led to different SC_i that were ratioed to the correct value in order to define an error, Diff=100.0*($SC_i - SC_{\text{true}}$)/SC_{true}.

For the sake of brevity the results for the neglect of both: RRS and VRS spectrum in the retrieval are not shown. This test showed the largest errors and non-acceptable fit residuals for all target species. The results are listed in Fig. 5.

First, the results for BrO are discussed in detail. Then, the corresponding studies for HCHO are discussed with respect to the results from the BrO retrievals.

7.2. BrO retrieval

In order to retrieve BrO all quantities for the DOAS evaluation were prepared in a wavelength range slightly larger than the fitting window of 344.7–359 nm which has been used for the retrieval of BrO from GOME data (Richter et al., 1998). SCIATRAN's model results were calculated including the absorption of O_3, NO_2, OClO, O_4, HCHO and BrO. The BrO SCs computed from the ODs of both scenarios are of comparable size.

7.2.1. Optical depth for scenario I:

Large errors (differences between actual SC and the true one) were found when neglecting the VRS compensation spectrum in the retrieval (test strategy 2). As anticipated in former sections, a Ring (RRS) spectrum is not capable to compensate for the lack of a VRS compensation spectrum because of the significantly different spectral structure of the processes.

However, visualization of BrO residuals showed that even at this error-level (−36.57%) the spectral signature of the species could still be found. Further tests with slant columns of the order of 10^{13} [molec cm^{-2}] showed that these structures could not be visualized anymore without taking VRS into account.

As demonstrated in an earlier publication (Vountas et al., 1998), trace gas retrievals can be significantly biased if a wrong Ring reference spectrum is used or even neglected (test strategy 3). This is of special importance for a minor trace gas such as BrO (Burrows et al., 1998). The neglect of RRS lead to errors of about 171%. Test strategy 4. shows a smaller error if a wrong scenario (II) is used for the computed reference spectra. Strategies 5 and 6 show that the reason for the error of 14% is almost completely related to the error in the RRS spectrum (test strategy 5) and not to the VRS

ACPD
3, 2931–2962, 2003

compensation spectrum (test strategy 6). Apparently a wrong assumption about VRS still leads to an improvement of the BrO SC.

7.2.2. Optical depth for scenario II:

The evaluation of the OD for scenario II revealed comparable results. However, neglecting VRS in the retrieval generates larger errors than in the previous scenario because of the stronger impact of VRS for small values of SZA and C (not shown).

As before, a wrong RRS spectrum leads to a larger error than wrong model assumptions for the VRS compensation spectrum (compare test strategy 1. and 5.-6.).

It should be noted that no significant differences could be found computing $I^{\pm VRS}$ with or without taking into account RRS. A direct comparison of r_w shows marginal differences. A DOAS retrieval of BrO using both types of VRS compensation spectra based on model data led to maximum errors in the retrieved slant column of less than 0.4%. The interaction of atmospheric RRS and oceanic VRS depends on a number of parameters. However, for most of the realistic GOME scenarios no significant error is expected. This has important consequences for computational speed, as model runs accounting for VRS but excluding RRS are significantly faster.

7.3. HCHO retrieval

All quantities used in the fit of HCHO were modeled using SCIATRAN for a wavelength window slightly larger than the fitting window of 337.35–356.12 nm that is used for HCHO retrieval from GOME (Wittrock et al., 2000). Absorption of O_3, NO_2, OClO, BrO, O_4 and HCHO has been taken into account.

The results are comparable to those of BrO. However, for both OD-scenarios neglecting VRS shows larger errors for HCHO as in case of BrO.

The omission of a Ring spectrum leads to the worst fit results. However, the introduction of wrong RRS and VRS spectra led to smaller errors compared to BrO retrieval. Again, wrong model assumptions for VRS were not provoking as large errors as the

same wrong assumptions in modeling of RRS.

8. BrO retrieval from GOME

In order to demonstrate the magnitude of the impact (not the error!) on measured data exemplarily, we have modeled a VRS spectrum for a SZA of 33° and included it in a DOAS fit on a series of consecutive GOME pixels located over oligotrophic ocean regions.

Figure 6 shows the results for clear-sky measurements from 1999 (orbit 19892). BrO was used as the target species. Reference spectra for NO_2, O_4 and O_3 for two temperatures were fitted together with a modeled Ring and VRS compensation spectrum at 33° SZA, and a under-sampling correction spectrum. A shift-and-squeeze of the wavelength axis of each spectrum relative to the GOME irradiance has been performed as part of the DOAS fit. r_r and r_w were computed with an adequate solar irradiance input from GOME.

In the upper plot BrO SCs are shown for the two cases, with (red) and without (black) VRS correction in the DOAS fit. The SC were plotted as a function of SZA (i.e. geolocation). The lower plot shows the relative difference between both results (Diff=100.0*($SC_{\mathrm{WithoutVRS}} - SC_{\mathrm{WithVRS}}$)/$SC_{\mathrm{WithVRS}}$). Differences between more than +20% and −5% can be observed. These values are below the theoretical ones shown in Fig. 5 which are about 36%, suggesting a higher chlorophyll concentration and therefore less impact on the OD.

Still, there are uncertainties on the impact of inaccurate absorption spectra of water in this wavelength region. An over-weighting of the impact of VRS on the retrievals might be the case.

We conclude, that taking into account a VRS compensation spectrum at small latitudes (small SZAs) will improve the accuracy of the SCs for BrO and comparable minor trace gases in GOME DOAS analyzes. However, the discrepancy between model and experimental data has still to be analyzed and is possibly related to inaccurately mod-

ACPD
3, 2931–2962, 2003

eled inherent optical properties of sea water.

A possible reason for the discrepancy could be the compensation of VRS spectral structures through 'shifting & squeezing' (relative wavelength calibration), as well as under-sampling correction spectra (especially relevant for GOME retrievals in the UV).

9. Conclusions

An simple ocean reflectance model introducing Vibrational Raman Scattering (VRS) as proposed by Sathendranath and Platt (1998) and Vasilkov et al. (2002b) has been incorporated in the atmospheric radiative transfer model SCIATRAN.

Model runs have been performed and the results have been qualitatively compared to results of another model. Good agreement could be found. The validation of the model against GOME data and those of dedicated measurements of the upwelling radiance above clear swimming pool water showed good results demonstrating that the model provides an adequate simulation of the effect.

A scheme was developed that is capable to compensate the impact of VRS on DOAS retrievals (similar to the compensation of the Ring effect) using a simple VRS compensation spectrum to be used as a pseudo absorber in the fit. This scheme is able to replace empirical approaches formerly used to reduce spectral signatures of VRS in DOAS retrievals.

In a sensitivity study, optical depths evaluated with model reference spectra showed promising results using a VRS compensation spectrum in order to correct for the impact of VRS. However, neglecting the effect led to large errors in the Slant Column (SC) for both minor trace gases investigated (BrO, HCHO). SC errors of 36 to over 100% could be observed.

However, either an over-estimation of the impact of VRS (due to potentially erroneous inherent optical properties) has been modeled or the impact of VRS on the retrieval of both gases from experimental data is compensated by shift & squeeze algorithms and under-sampling correction spectra.

Similar behavior will usually not have to be expected for OClO even though it is commonly retrieved in the critical UV wavelength region. The gas is evaluated only at high solar zenith angles and mostly in polar regions where chlorophyll levels tend to be higher and therefore the impact of VRS is not expected to be large.

The introduction even of a compensation spectrum modeled under wrong assumptions provides significantly smaller errors in the model tests for both investigated gases. This makes the VRS compensation spectrum a promising and simple tool to optimize the GOME DOAS fits at low latitudes.

A similar impact can be expected also for forthcoming missions like GOME-2 and OMI, as well as for the already deployed instrument SCIAMACHY.

Future work comprises the introduction of improved input parameters for the reflectance model and a feasibility study to retrieve chlorophyll-a concentrations using the VRS compensation spectrum with DOAS.

Acknowledgement. The authors would like to thank the SeaWiFS Project and the Goddard Earth Sciences Data and Information Services Center/Distributed Active Archive Center for the distribution of the SeaWiFS data. We thank V. V. Rozanov and R. de Beek for stimulating discussions and critical reading of the manuscript. M. Vountas would like to thank A. Vountas for inspiration.

References

Bartlett, J., Voss, K., Sathyendranath, S., and Vodacek, A.: Raman scattering by pure water and seawater, Appl. Opt., 37, 1998. 2941

Brühl, C. and Crutzen, P.: Chemo-dynamical model of the atmosphere: Profile data base, personal communication, 1992. 2942, 2947

Burrows, J., Eisinger, M., and Vountas, M.: Design, Development and Upgrading of Prototype Software Tools for Use with ESRIN Atmopheric Reference Processor, Tech. rep., ESRIN Report, ESRIN Contract 12030/96/I-H-GE, 1998. 2949

Burrows, J. P., Weber, M., Buchwitz, M., Rozanov, V., Ladstätter-Weißenmayer, A., Richter, A., de Beek, R., Hoogen, R., Bramstedt, K., Eichmann, K.-U., Eisinger, M., and Perner, D.: The

Global Ozone Monitoring Experiment (GOME): Mission concept and first scientific results, J. Atmos. Sci., 56, 151–175, 1999. 2933
de Beek, R., Vountas, M., Rozanov, V., Richter, A., and Burrows, J.: The Ring effect in the cloudy atmosphere, Geophys. Res. Let., 28, 2001. 2934
Ge, Y., Gordon, H., and Voss, K.: Simulation of inelastic-scattering contributions to the irradiance field in the ocean: variation in Fraunhofer line depths, Appl. Opt., 32, 1993. 2941
Grainger, J. and Ring, J.: Anomalous Fraunhofer line profiles, Nature, 193, 762, 1962. 2933
Haltrin, V. and Kattawar, G.: Self-consistent solution to the equation of radiative transfer with elastic and inelastic scattering in ocean optics: 1 model, Appl. Opt., 32, 1993. 2933, 2935, 2941
Kattawar, G. and Xu, X.: Filling in of Fraunhofer lines in the ocean by Raman scattering, Appl. Opt., 30, 1992. 2941
Kattawar, G., Young, A., and Humphreys, T.: Inelastic scattering in planetary atmospheres, I, the Ring effect, without aerosols, Astrophys. J., 243, 1049–1057, 1981. 2933
Kneizys, F., Shettle, E., Abreu, L., Chetwynd, J., Anderson, G., Gellery, W., Selby, J., and Clough, S.: Users Guide to LOWTRAN 7, Tech. Rep. AFGL-TR-86-0177, Air Force Geophys. Lab., Hanscom AFB, Mass., 1986. 2942, 2947
Kurucz, R., Furenlid, I., Brault, J., and Testerman, L.: Solar flux atlas from 296 to 1300 nm, Tech. rep., National Solar Observatory, Sunspot, New Mexico, 1984. 2945, 2947
Marshall, B. and Smith, R.: Raman scattering and in-water ocean optical properties, Appl. Opt., 29, 1990. 2933
Mobley, C.: Light and Water-Radiative Transfer in Natural Waters, Academic Press, 1994. 2938
Morel, A.: Optical modeling of the upper ocean in relation to its biogeneous matter content (case i waters), J. Geophys. Res., 93, 1988. 2940
Morel, A. and Prieur, L.: Analysis of variations in ocean color, Limnol. Oceanogr., 22, 1977. 2937
Patterson, K. W.: Contribution of chromophoric dissolved organic matter to attenuation of UV radiation in three contrasting coastal areas, PHD work, UCLA, Santa Barbara, 2000. 2940
Platt, U. and Perner, D.: Direct measurement of atmospheric HCHO, HNO_2, O_3, NO_2 and SO_2 by differential optical absorption spectroscopy, J. Geophys. Res., 85, 1980. 2934
Pope, R. and Fry, E.: Absorption spectrum (380-700nm) of pure water. ii. integrating cavity measurements, Appl. Opt., 36, 1997. 2940
Quickenden, T. and Irvin, J.: The ultraviolet absorption spectrum of liquid water, J. Chem. Phys.,

72, 1980. 2940
Richter, A. and Burrows, J.: A multi wavelength approach for the retrieval of tropospheric NO_2 from GOME measurements, in proceedings of the ERS-ENVISAT symposium, Gothenburg October 2000, ESA publication SP-461, 2000. 2935
Richter, A., Wittrock, F., Eisinger, M., and Burrows, J. P.: GOME observations of tropospheric BrO in northern hemispheric spring and summer 1997, Geophys. Res. Lett., 25, 2683–2686, 1998. 2949
Rozanov, V., Diebel, D., Spurr, R., and Burrows, J.: GOMETRAN: A radiative transfer model for the satellite project GOME – the plane-parallel version, J. Geophys. Res., 1997. 2934, 2942
Sathendranath, S. and Platt, T.: Ocean-color model incorporating transspectral processes, Appl. Opt., 37, 1998. 2932, 2933, 2934, 2935, 2937, 2938, 2939, 2952
Smith, R. and Baker, K.: Optical properties of the clearest natural waters (200-800nm), Appl. Opt., 20, 1981. 2941
Solomon, S., Schmeltekopf, A. L., and Sanders, R. W.: On the interpretation of zenith sky absorption measurements, J. Geophys. Res., 92, 8311–8319, 1987. 2944
Stavn, R. and Weidemann, A.: Optical modeling of clear ocean light fields: Raman scattering effects, Appl. Opt., 27, 1988. 2933
Vasilkov, A., Herman, J., Krotkov, N., Kahru, M., Mitchell, B., and Hsu, C.: Problems in assement of the ultraviolet penetration into natural waters from space-based measurements, Opt. Eng., 41, 2002a. 2940
Vasilkov, A. P., Joiner, J., Gleason, J., and Bhartia, P.: Ocean Raman scattering in satellite backscatter UV measurements, Geophys. Res. Let., 10, 2002b. 2933, 2934, 2936, 2937, 2939, 2940, 2943, 2952
Vountas, M.: Modeling and Parameterization of the Ring Effect: Impact on the retrieval of stratospheric Trace Gases-PHD work In German, ISBN 3-8265-4649-0, Shaker, 1998. 2934
Vountas, M., Rozanov, V., and Burrows, J.: Ring effect: Impact of rotational Raman scattering on radiative transfer in earth's atmosphere, J. Quant. Spectrosc. Radiat. Transfer, 60, 943–961, 1998. 2933, 2934, 2935, 2936, 2942, 2949
Walrafen, G.: Raman spectral studies of the effects of temperature on water structures, J. Chem. Phys., 47, 1967. 2941
Wittrock, F., Richter, A., Ladstätter-Weißenmayer, A., and Burrows, J. P.: Global observations of formaldehyde, in proceedings of the ERS-ENVISAT symposium, Gothenburg October 2000, ESA publication SP-461, 2000. 2935, 2950

Young, A.: Rayleigh scattering, Phys. Today, 1982. 2938

ACPD

3, 2931–2962, 2003

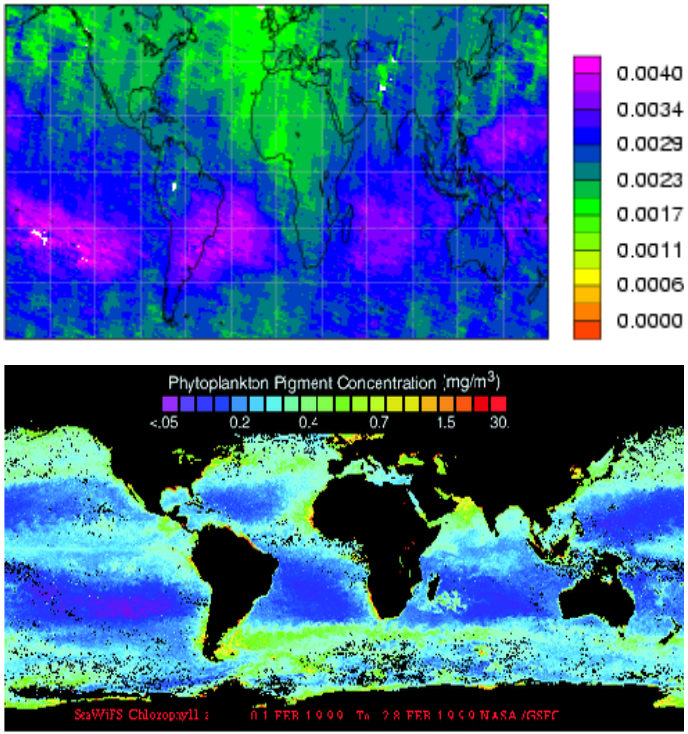

Fig. 1. Above: GOME fit quality results plotted for February 1999; below: Chlorophyll-a concentration from SeaWiFS for the same period.

ACPD

3, 2931–2962, 2003

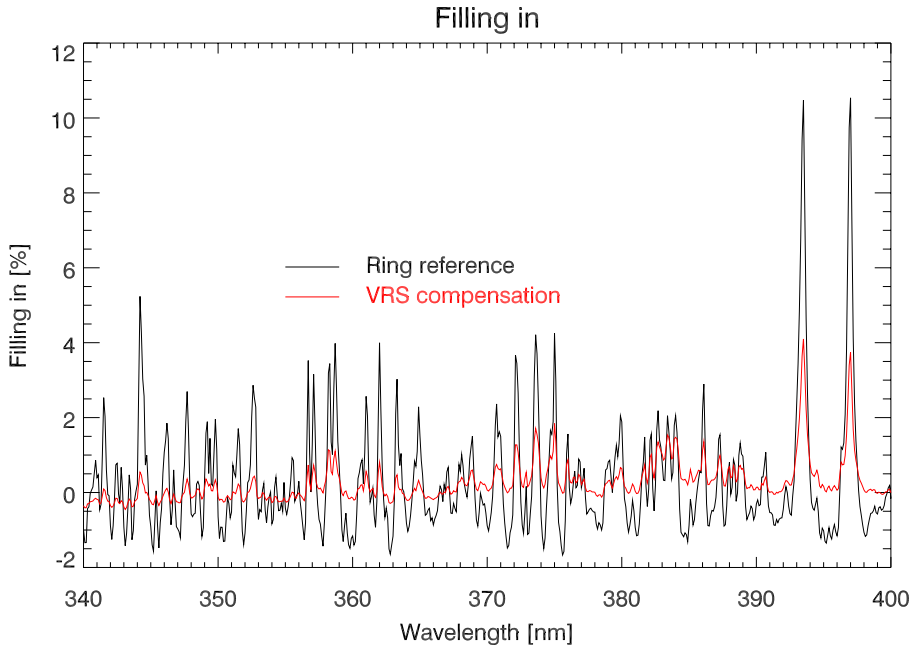

Fig. 2. Comparison of Ring reference and VRS compensation spectrum as defined in Eq. (2).

ACPD
3, 2931–2962, 2003

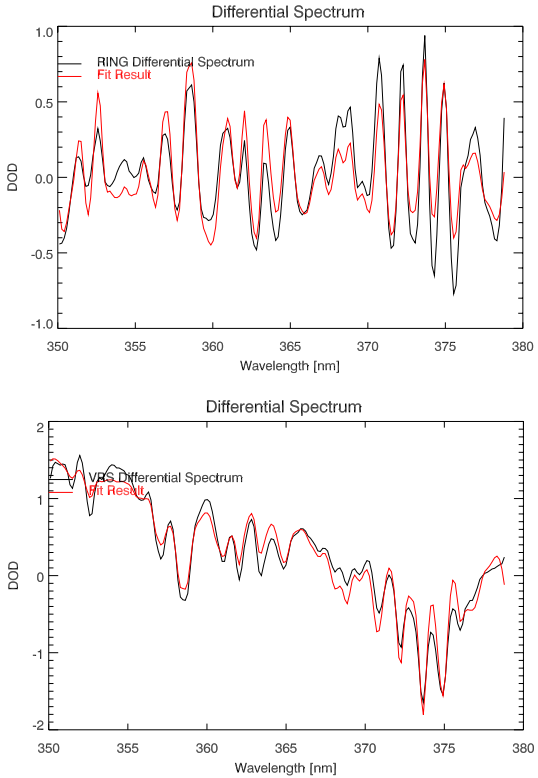

Fig. 3. Fitting of Swimming pool data. Above: Fit results for Ring reference spectrum; below: Fit results for VRS compensation spectrum.

ACPD
3, 2931–2962, 2003

Inelastic scattering in ocean water

M. Vountas et al.

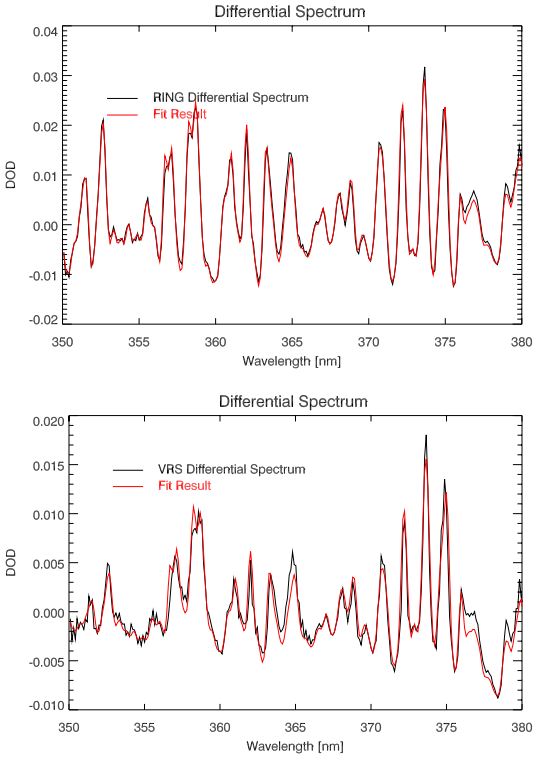

Fig. 4. DOAS fits of clear-sky GOME data (Level 1 filename: 90208175). Above: Fit results for Ring reference spectrum; below: Fit results for the VRS compensation spectrum.

ACPD
3, 2931–2962, 2003

Scenario I: SZA=50°, C=0.01 — Scenario II: SZA=30°, C=0.001

BrO Slant Column [10^{14} molec cm^{-2}] — AMF-I: ~2,2

Optical Depth (OD)	1. RRS-I VRS-I		2. RRS-I No VRS		3. No RRS VRS-I		4. RRS-II VRS-II		5. RRS-I VRS-II		6. RRS-II VRS-I	
	SC	Diff [%]	SC	Diff [%]	SC	Diff [%]	SC	Diff [%]	SC	Diff [%]	SC	Diff [%]
OD-I with RRS-I/VRS-I	5,09	0,00	3,23	-36,57	13,79	171,14	5,79	13,80	5,07	-0,24	5,78	13,63
OD-II with RRS-II/VRS-II	3,68	-14,49	1,53	-64,48	11,51	167,36	4,31	0,00	3,66	-14,98	4,32	0,35

HCHO Slant Column [10^{16} molec cm^{-2}] — AMF-I: ~1,6

Optical Depth (OD)	1. RRS-I VRS-I		2. RRS-I No VRS		3. No RRS VRS-I		4. RRS-II VRS-II		5. RRS-I VRS-II		6. RRS-II VRS-I	
	SC	Diff [%]	SC	Diff [%]	SC	Diff [%]	SC	Diff [%]	SC	Diff [%]	SC	Diff [%]
OD-I with RRS-I/VRS-I	7,67	0,00	13,40	74,71	-112,40	-1565,45	8,09	5,49	7,66	-0,14	8,11	5,75
OD-II with RRS-II/VRS-II	6,72	-5,65	12,86	80,64	-102,50	-1539,81	7,12	0,00	6,71	-5,79	7,13	0,21

Fig. 5. Slant column fitting results. Errors were defined as e=100.0*($SC_{\text{Retrieved}}$ – $SC_{\text{WithtrueVRS}}$)/$SC_{\text{WithtrueVRS}}$.

ACPD
3, 2931–2962, 2003

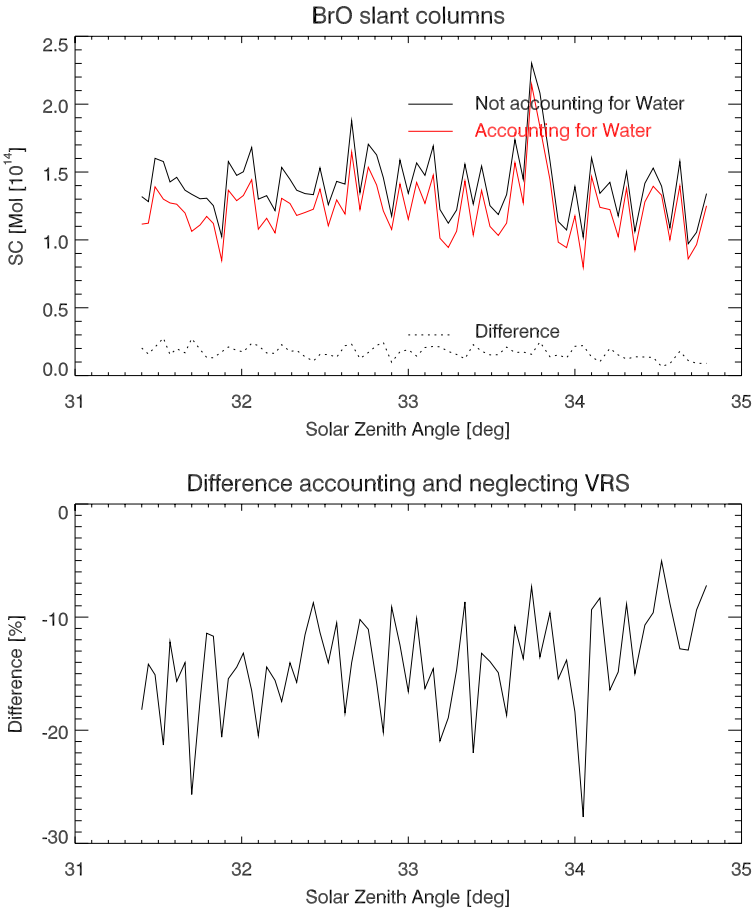

Fig. 6. DOAS fits of clear-sky GOME data (Level 1 filename: 90208175).

ACPD
3, 2931–2962, 2003